Removal of Cd(II) from water using zero valent iron/copper functionalized spent tea

Khan Malook and Hamayun Khan

ABSTRACT

Zero valent Fe/Cu functionalized spent tea adsorbent was prepared for the decontamination of Cd(II) contaminated water. The synthesized material was characterized for structural and morphological characteristics using various analytical techniques. The material was used as adsorbent for the adsorption of Cd(II) from aqueous solutions in batch study experiments. The effect of initial pH, adsorbent dosage, contact time and adsorbate concentration was investigated. The obtained data well followed the Langmuir adsorption isotherm model and pseudo-second order rate model with maximum adsorption capacity of 89.686 mg·g^{-1}. Based on Langmuir separation factor (R), having a value of 0.706–0.194, the adsorption process was confirmed to be favorable. The adsorbent was used in the form of a column for the sorption of Cd(II) from a running solution with satisfactory results. The spent material was regenerated and reutilized with reduction of adsorption capacity by 1.48% only. Overall, the current adsorbent can be efficiently utilized for the removal of aqueous Cd(II).

Key words | adsorption capacity, FTIR, monolayer, separation factor, STP-ZVI/Cu

Khan Malook (corresponding author)
Centralized Resource Laboratory,
University of Peshawar,
Peshawar 25120,
Pakistan
E-mail: *malook.btni@yahoo.com*

Hamayun Khan
Department of Chemistry,
Islamia College Peshawar,
Peshawar 25120,
Pakistan

HIGHLIGHTS

- Zero valent iron/copper functionalized spent tea composite was successfully prepared to get rid of the deficiencies faced by individual materials.
- The composite material was applied for the removal of Cd(II) from water with encouraging results.
- The adsorbent has maximum adsorption capacity of 89.686 mg·g^{-1}.
- The material can be regenerated and reutilized with small reduction in the adsorption capacity.

INTRODUCTION

Water is an important and essential component of the Earth for life's existence and is known as a universal solvent due its capability to dissolve a large number of different compounds. However, this capability of water is disastrous to some extent as it is easily exposed to pollutants. Toxic substances such as fertilizers, pesticides, dyes, oils, microplastics etc. from farms, towns, fields, and factories can easily dissolve/mix with running water, causing water pollution (Sharma *et al.* 2019).

Heavy metal ions are among the most important groups of pollutants responsible for water contamination. They are widely used in various industrial processes such as pesticides, fertilizers, mining, batteries, refining ores, electroplating, tanneries etc. (Peng *et al.* 2018), from where they are subsequently released into the water bodies which results in hazardous aquatic ecosystems and human health problems. They are nonbiodegradable and enter into the human body through various channels such as food chains and drinking water and causing nerve, kidney, cardiovascular, dementia, and liver diseases (Ahmed *et al.* 2017). Some heavy metals such as Zn, Cu, Fe, etc. have important biological functions and are needed for the human body below

doi: 10.2166/wst.2020.527

certain permissible limits (Koury *et al.* 2007). However, metals like Cd, Pb, and Cr have no specific function in the human body and are extremely toxic. These heavy metals accumulate in different parts of the body and create various health problems.

Cd(II) is an extremely toxic metal and is used in electroplating, pigment works, photography, and metallurgical alloying. The maximum contaminated level (MCL) for Cd is 0.01 mg/L (Barakat 2011). Exceeding the Cd(II) level beyond MCL is highly risky because of its greater half-life and ability to make stable coordinate complexes with biomolecules, thereby effecting their normal functioning. Cd(II) effects kidneys leading to insufficiency of renal function, damaging liver and also causes osteoporosis (Lin *et al.* 2015). Therefore, timely exclusion of Cd(II) from waste water is utmost important.

Various methods such as ion exchange, precipitation, reverse osmosis, adsorption, flocculation, and membrane separation are in practice for the removal of heavy metal ions from waste water. Among these methods, the adsorption process is considered to be highly efficient and economical. Therefore, the researchers have a keen interest in the application of adsorption methods for removal of heavy metal ions from waste water. The adsorbents, particularly based on agricultural wastes, have been widely used for this purpose due to their mass production and cost–effectiveness.

Currently spent black tea has gained immense attention as an economical adsorbent for removal of pollutants from waste water. A huge quantity of black tea is used in tea shops, restaurants, and house kitchens every day and is disposed unutilized. Tea leaves have insoluble cell walls mostly composed of cellulose, hemicellulose, lignin, condensed tennis and structural proteins with variety of functional groups such as carboxylate, aromatic carboxylate, phenolic hydroxyl which are capable of up taking the contaminants. Due to these characteristics, spent tea is used for the extraction of heavy metal ions from water (Zuorro & Lavecchia 2010).

However, using agricultural waste-based adsorbents without any modification may suffer from several drawbacks such as poor adsorption capacity, lack of specificity and smaller durability. Therefore, proper modification of these adsorbents is needed to improve their performance.

Some of the researchers have reported the application of zero valent metal nanoparticles for the sorption of heavy metal ions from waste water (Mu *et al.* 2017). For example, Shubair *et al.* (2018) reported the application of Fe nanoparticles (Fe NP) and bimetallic Fe/Cu nanoparticles for waste water treatment due to their higher surface area, nontoxicity and ease of synthesis. The materials were observed to have high affinity to various pollutants from waste water. However, the adsorption capacity of materials like these is compromised due to their oxidation and agglomeration (Harman & Genisoglu 2016). Similarly, nanomaterials also face the problem of filtration due to their smaller particle size. These hurdles can be removed by loading metal nanoparticles on to supporting material like agricultural waste (Ponmani & Udayasoorian 2013). In such types of composite adsorbents, both the metallic nanoparticles and agricultural waste play their role in the removal of contaminants from waste water.

Thus, in the present study, we attempted to prepare a composite adsorbent based on zero valent Fe/Cu/spent black tea powder to get rid of the deficiencies faced by individual materials and add up their individual characteristics. After successful synthesis, the material was used as an effective adsorbent for the remediation of Cd(II) contaminated water at various experimental conditions. Furthermore, isotherm and kinetics studies were carried out to examine the performance of the adsorbent.

MATERIALS AND METHOD

Materials

Chemicals like HCl, NaOH, $FeCl_3{\cdot}6H_2O$, $Cu(NO_3)_2{\cdot}3H_2O$ and $Cd(NO)_3$ were used in this study. HCl was of general reagent grade while the rest of the reagents such as NaOH, $FeCl_3{\cdot}6H_2O$, $Cu(NO_3)_2{\cdot}3H_2O$ and $Cd(NO)_3$ were of analytical grade, which were procured from Sigma-Aldrich (Germany) through local suppliers. The stock standard solution (1,000 mg/L) of Cd(II) was prepared by dissolving suitable amount of $Cd(NO)_3$ in distilled water. Milli-Q water (18.25 $M\Omega{\cdot}cm^{-1}$) was used for the preparation of solutions.

Preparation of adsorbent

The adsorbent was prepared in the following two steps.

Step-1: First, a sufficient quantity of spent tea (ST) was collected from home kitchen. The collected tea (30 g) was washed with copious amount of tap water followed by rinsing with distilled water to eliminate all types of removable colors. After sun drying, the ST was kept soaked in 0.5 M NaOH solution overnight to eradicate the remaining colors followed by rinsing with distilled water until neutral pH of the cleaning water was obtained.

This product was oven dried (60 °C) and crushed to fine powder using fruit blender and named as spent tea powder (STP).

Step-2: The STP (15 g) was added into a beaker having 100 mL (0.01 M) solution of $FeCl_3{\cdot}6H_2O$ and $Cu(NO_3)_2{\cdot}3H_2O$ and magnetically stirred for 2 hours for possible chelation of metal ions with the STP functional groups. In the meanwhile, 10.0 g of green tea was heated in 100 mL deionized water for 1 h at 80 °C followed by filtration to obtain green tea extract (GTE). Then, 50 mL of the GTE was gradually dropped into the STP mixture with $FeCl_3{\cdot}6H_2O$ and $Cu(NO_3)_2{\cdot}3H_2O$ in a nitrogen atmosphere. Soon after adding GTE, the mixture converted into a product of intense black color, which indicated the conversion of Fe(III) and Cu(II) into zero valent state (Gopal *et al.* 2020). The stirring was continued for 20 minutes. Afterward, the liquid part of the mixture was removed by decantation. The product was rinsed with deionized water by decantation and then filtration to ensure the removal of free zero valent Fe and Cu. The final product was vacuum dried and named as STP-ZVI/Cu.

Point zero charge (PZC) of the adsorbent

The pH PZC of the current adsorbent was determined according to the reported procedure (Bagheri *et al.* 2012; Rahim 2018) with some modifications. In a typical experiment, 20 mL of distilled water was taken in a series of beakers and the pH was adjusted in the range of 2.0–9.0 using concentrated solution of HNO_3 or NaOH. Afterward, 5 mL of each of the solutions (Milli-Q water of known pH) was taken in a series of test tubes followed by adding exactly 0.5 g of the adsorbent. The test tubes were shaken for 24 h at room temperature and then the final pH of the solutions was measured.

Characterization

STP-ZVI/Cu was characterized for various characteristics. The structural analysis was carried out by Fourier transform infrared spectroscopy (FT-IR-8400, Shimadzu, Japan) from 400–4,000 cm^{-1}. The surface morphology was examined by using scanning electron microscopy (SEM) (JSM5910, Joel, Japan). The content of zero valent metals or their oxides were identified via X-ray diffractometry (JEOL JDX-9C_XRD, Japan). The concentration of Cd(II) and content of ZVI/Cu in STP-ZVI/Cu were determined by atomic absorption spectrometry (AAS) (AAnalyst 700, Perkin Elmer USA).

Adsorption study

Cd(II) adsorption characteristics of the adsorbent were investigated by batch study experiments where a known quantity of STP-ZVI/Cu was added into a known volume of Cd(II) solution in a conical flask. The mixture was magnetically stirred for fixed intervals of time. Afterward, the adsorbent was separated by filtration via Whatman filter paper No. 42 and concentration of the analyte was determined. Equations (1) and (2) was used to determine the Cd(II) absorptivity and percent removal efficiency of the adsorbent respectively:

$$q_e = \frac{(C_o - C_e)V}{m} \tag{1}$$

$$\eta_{\%} = \frac{(C_o - C_e)}{C_o} \times 100 \tag{2}$$

In the above relation 1 and 2, q_e ($mg{\cdot}g^{-1}$) represent adsorption capacity, C_o ($mg{\cdot}L^{-1}$) is the initial concentration, C_e ($mg{\cdot}L^{-1}$) indicates residual concentration, V(L) is the volume of solutions, m (g) is the weight of adsorbent and η% is the percent removal efficiency.

RESULTS AND DISCUSSION

Characterization of the adsorbent

Bioadsorbents have various functional groups on their surfaces necessary for metal ions' uptake. To confirm the presence of these functional groups, FTIR analysis of both STP and STP-ZVI/Cu was carried out and the result is presented in Figure 1(a) and 1(b). FTIR spectrum of STP has

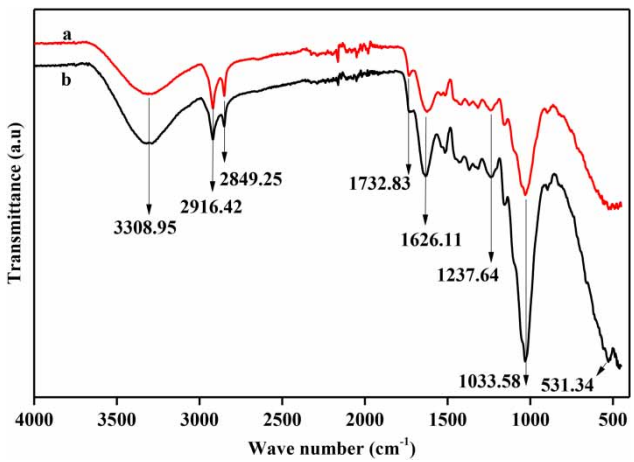

Figure 1 | FTIR spectra of (a) STP, (b) STP-ZVI/Cu.

absorption bands at 3,308.95, 2,916.42, 2,849.25, 1,732.83, 1,626.11, 1,237.64 and 1,033.58 cm^{-1}. The band at 3,308.95 cm^{-1} is assigned to O-H stretching vibrations. The bands at 2,916.42 and 2,849.25 cm^{-1} are assigned to the stretching vibration of aliphatic C-H group (Wen *et al.* 2017). The peaks at 1,732.83 and 1,626.11 cm^{-1} are due to the presence of C = O functional group. The bands at 1,242.53 cm^{-1} and 1,033.58 cm^{-1} are allocated to C-O and C-N bonds stretching respectively (Silverstein *et al.* 2014). Thus, FTIR study confirms the presence of functional groups necessary for the uptake of Cd(II). The FTIR spectrum of STP-ZVI/Cu (Figure 1a, b) has all the bands of STP, indicating that ZVI/Cu has no effect on the chemical composition of STP. Further, in the case of STP-ZVI/Cu, the peaks for the existence of Cu_2O or CuO were not detected. Similar result was also reported by Mahmoud *et al.* (2020). The peak at 531.34 cm^{-1} is assigned to Fe-O bonds (Zhang *et al.* 2011). This may be due to the conversion of some of the ZVI into oxide form.

Surface morphology

Surface morphology of an adsorbent plays an important role in the adsorption process. Bioadsorbents have porous surfaces that enhance their adsorption efficiency. The surface morphology of STP and STP-ZVI/Cu was investigated with scanning electron microscopy and the result is depicted in Figure 2(a)–2(c). The images were taken at different magnifications to observe the effect of ZVI/Cu on STP. The agglomerates in Figure 2(c) are related to the zero valent Fe, Cu and their oxides. The functionalized STP is of porous and rough surface compared to the parent STP which may be the effect of soaking solution (NaOH solution) or other reactants such as $FeCl_3{\cdot}6H_2O$, $Cu(NO_3)_2{\cdot}3H_2O$. Such porous materials have greater surface area where more active sites are available for adsorbate particles. The adsorbate particles can easily enter into the pores and attach to the active sites (Malook & Haque 2019).

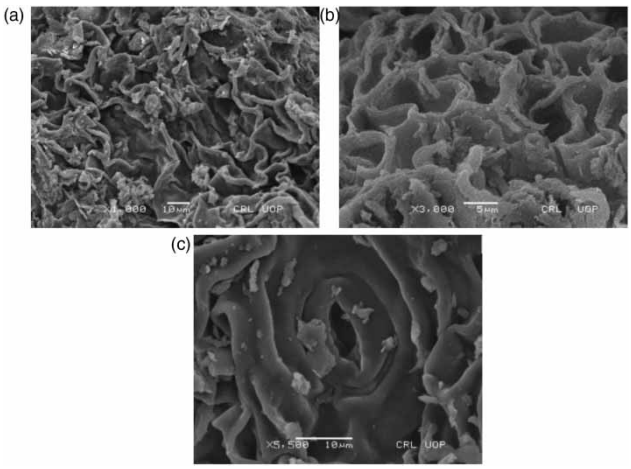

Figure 2 | SEM images of (a) STP, (b, c) STP-ZVI/Cu.

X-ray diffractometry

X-ray diffractometry of STP and STP-ZVI/Cu is presented in Figure 3(a) and 3(b). As per XRD analysis, STP is amorphous while the diffractogram of STP-ZVI/Cu has sharp peaks of Cu at 2θ position of 44° and 52° (JPCDS 89-2838) Huang *et al.* (2012). The peaks at 2θ position of 35 and 65° (JPCDS 05-0667) are assigned to CuO. Thus, XRD analysis proved the presence of Cu and CuO in the final product. No distinct peak related to ZVI were identified, which may be due to the amorphous structure of ZVI (Wei *et al.* 2017).

Content of Fe/Cu in the adsorbent

To determine the actual content of Fe/Cu in the adsorbent, 0.09 g of STP-ZVI/Cu was added into a conical flask, followed by 10 mL of concentrated HNO_3, and was allowed to stand overnight. Afterward, the mixture was gently heated on a hotplate until the production of red fumes (NO_2) ended. After cooling, 5 mL of concentrated $HCLO_4$ was added and heated to evaporate to a small volume. The final solution was diluted with deionized water up to 50 mL. The concentration of Fe and Cu in the final solution was determined by AAS. The content of Fe and Cu was 11.86 mg/g and 1.73 mg/g respectively. The relatively smaller

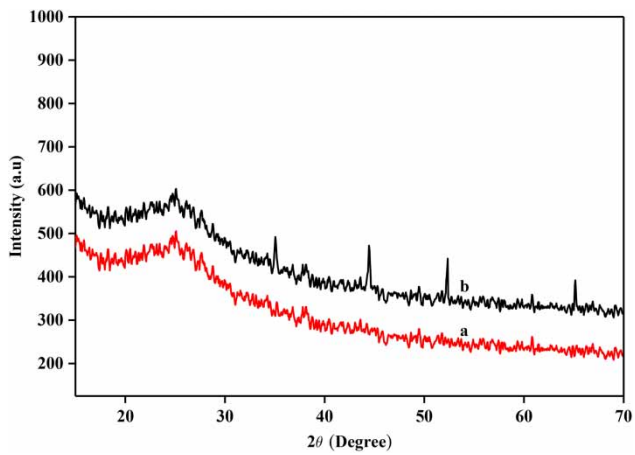

Figure 3 | XRD patterns of (a) STP, (b) STP-ZVI/Cu.

content of Cu may be due to the relatively poor efficiency of GTE to convert $Cu(NO_3)_2{\cdot}3H_2O$ into zero valent copper.

pH_{PZC} of STP-ZVI/Cu

The point of zero charge (pH_{PZC}) is the point at which the adsorbent surface becomes electrically neutral. At $pH < pH_{PZC}$, the adsorbent surface is positively charged and is suitable for uptake of anionic species, while at $pH > pH_{PZC}$, the surface of the adsorbent has negative charge and uptakes positively charged cationic species. For pH PZC determination, the value of the initial pH of the solution was plotted against the difference in the final and initial pH ($\Delta pH = pH_{final} - pH_{initial}$) as shown in Figure 4. The point of zero charge was determined from the point where it intersected the $\Delta pH = 0$ i.e. $pH_{final} = pH_{initial}$. The pH_{PZC} was found to be 5.0. Thus, the adsorbent is suitable to be used for Cd(II)) at pH greater than 5 where it has a negatively charged surface.

Adsorption study

pH effect

pH is a key parameter influencing the absorptivity of an adsorbent (Gong & Tang 2020). The effect of pH on the sorption capacity of STP-ZVI/Cu was studied in the pH range 3 to 8 and the result is exhibited in Figure 5. The adsorbent has a sorption capacity at lower pH that enhances with increase in pH. This may be due to the fact that at lower pH, the surface of the adsorbent is positively charged due to the higher concentration of H^+ (from HNO_3), which competes with Cd(II)

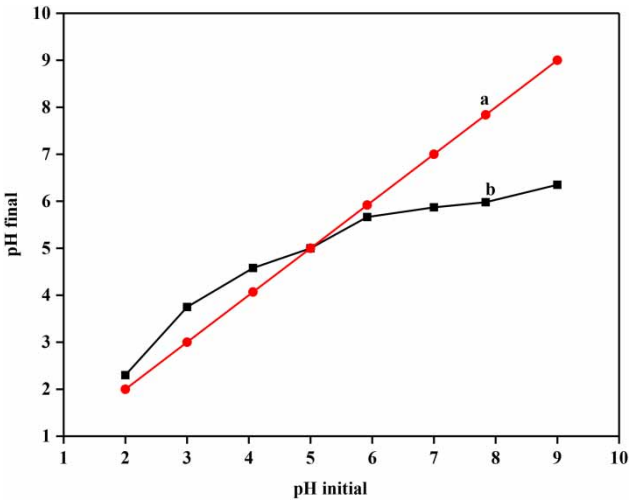

Figure 4 | Point of zero charge (pH_{PZC}) of STP-ZVI/Cu (a) pH initial vs pH final, (b) pH final-pH initial.

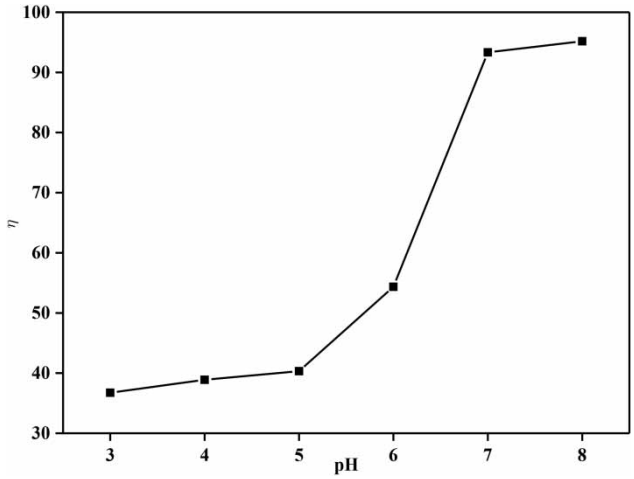

Figure 5 | Effect of solution pH on the adsorption capacity of STP-ZVI/Cu.

for binding to the available adsorption sites of the adsorbent. Thus, the adsorption of Cd(II) is restricted because of electrostatic repulsion (Liu *et al.* 2018). As the pH of the solution increases; that is, the concentration of H^+ decreases, more and more active sites become available for Cd(II) ion attachment due to the deprotonation of functional groups and hence the sorption capacity of the adsorbent enhances. The maximum sorption capacity of the adsorbent was achieved at pH 7 (93%) and 8 (94%). However, we preferred to use pH 7 for onward study because at higher pH (8 and above), there is the possibility of metal ion precipitation in the form of hydroxides (Goyal *et al.* 2001) where there is no input of adsorbent. The pH study on the adsorption capacity of STP-ZVI/Cu is in line with pH_{PZC} results.

Shaking time

A known quantity of adsorbent (0.2 g) was shaken with 20 mL (30 $mg{\cdot}L^{-1}$) of Cd(II) solution at pH 7 for 5–60 minutes and the result is depicted in Figure 6. The concentration of the adsorbate in the solution was found to decrease rapidly with shaking time. Maximum sorption was obtained at 40 minutes with no appreciable change afterward. Initially, there is greater difference between the concentration of Cd(II) in the surrounding solution and the solid-liquid interface. Thus, the Cd(II) rapidly attached to the available adsorption sites on the adsorbent surface. Later on, this difference of concentration decreases as most of the adsorption sites get occupied and hence the sorption capacity of the adsorbent also declines (Pillai *et al.* 2013). Thus, the adsorption equilibrium was achieved at 40 minutes which was used as optimum time for onward experiments.

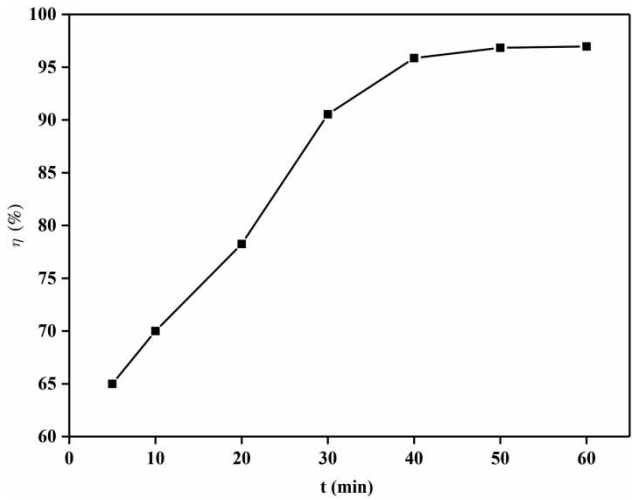

Figure 6 | Variation of adsorption capacity of STP-ZVI/Cu with shaking time.

Effect of adsorbent amount

Variation of the adsorption capacity of the adsorbent was studied by adding 0.05 to 0.30 g of the adsorbent to 20 mL (30 mg·L^{-1}) of Cd(II) solution at pH 7. The sorption capacity was found to increase with adsorbent dosage, as depicted in Figure 7. Maximum concentration of Cd(II) was removed by 0.15 g of the adsorbent. The absorptivity of an adsorbent depends on the availability of active sites, which increase with increase in the adsorbent dosage. At 0.15 g of the adsorbent, there established an equilibrium between metal ion concentration in the solution and liquid-solid interphase. To keep the equilibrium constant, additional Cd(II) cannot adsorb on the adsorbent surface in spite of the availability of more adsorption sites at higher adsorbent dosage. Therefore, the adsorbent dosage has no effect on adsorbate removal after 0.15 g. Thus, 0.15 g was considered as optimum weight for the maximum removal of Cd(II) at the current experimental conditions.

Effect of adsorbate concentration

The effect of initial concentration on the adsorption capacity of STP-ZVI/Cu is illustrated in Figure 8. The concentration of solution was varied from 5 to 50 mg·L^{-1} at optimum pH, contact time and adsorbent dosage. As the figure shows, the removal efficiency of the adsorbent decreases from ~97–90% with Cd(II) concentration. As the concentration of Cd(II) increases, more and more ions of the adsorbate attach to the adsorbent surface and the adsorption sites get occupied. As a result, Cd(II) uptaking efficiency of the adsorbent declines (Gaya *et al.* 2015).

Adsorption isotherms

For adsorption isotherm study, several equilibrium models have been developed (Foo & Hameed 2010). Langmuir and Freundlich adsorption isotherm models are commonly in practice. So the data obtained from the effect of the concentration study was fitted to the Langmuir and Freundlich adsorption isotherm models.

Langmuir adsorption model: This model suggests:

(i) Monolayer coverage of the adsorbent surface with no interaction among the adsorbate molecules or ions.
(ii) The adsorbent surface is homogenous and adsorption sites are equally accessible.

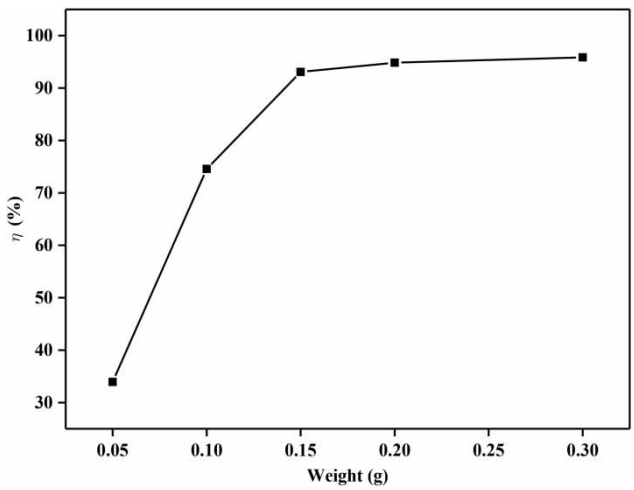

Figure 7 | Variation of adsorption capacity of STP-ZVI/Cu with adsorbent dosage.

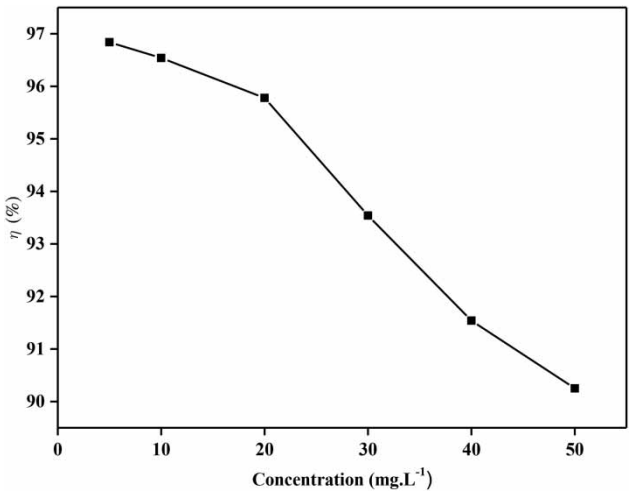

Figure 8 | Variation of adsorption capacity of STP-ZVI/Cu with adsorbate concentration.

(iii) Maximum adsorption occurs when the adsorbent surface is covered by a monolayer of adsorbate molecules/ions

The linear form of the Langmuir equation is given in Equation (3) (Gupta *et al.* 2017):

$$\frac{1}{q_e} = \frac{1}{bq_eC_e} + \frac{1}{q_m} \tag{3}$$

where q_e and C_e have already been explained in Equation (1) and 2 q_m(mg·g^{-1}) is related to monolayer adsorption capacity and b (L·mg^{-1}, the Langmuir equilibrium constant) is the affinity of the adsorbent towards the adsorbate. Based on Langmuir adsorption isotherm plot for Cd(II) ions (Figure 9), the value of q_m and b is 89.686 (mg·g^{-1}) and 0.083 (L·mg^{-1}) respectively with regression coefficient (R^2) 0.999. Another important characteristic of the Langmuir adsorption isotherm can be better explained by separation factor 'R' which provide information about the favorability of adsorption process and is given by Equation (4):

$$R = \frac{1}{(1 + bC_0)} \tag{4}$$

The value of 'R' is from 0.706–0.194 for all initial concentration values indicating that in the present case, adsorption of Cd(II) on STP-ZVI/Cu is a favorable process (Sen *et al.* 2010).

Freundlich model: This model proposes:

(i) Monolayer adsorption with heterogeneous distribution of functional groups.
(ii) Interaction among the adsorbate molecules or ions.

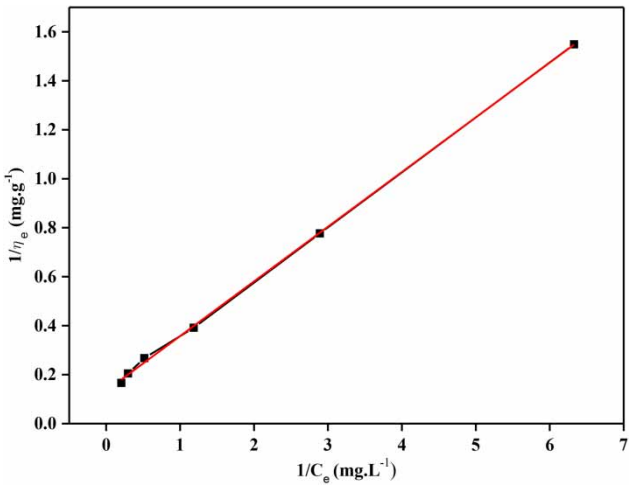

Figure 9 | Langmuir adsorption isotherm for Cd(II) ions removal by STP-ZVI/Cu.

(iii) The linear form of the Freundlich equation is given in Equation (5) (Baldermann *et al.* 2018):

$$\log q_e = \log K_f + \frac{1}{n}\log C_e \tag{5}$$

where n and K_f are the sorption intensity and capacity respectively. The plot of log q_e vs. log C_e is presented in supplementary data (Figure S1 in Supplementary Material). The relatively smaller R^2 value (0.978) for the Freundlich isotherm shows that the Langmuir isotherm model can better fit the experimental data. As discussed earlier, the Langmuir isotherm model suggests monolayer adsorption of adsorbate on the surface of adsorbent indicating that the Cd(II) ions were monolayer adsorbed on STP-ZVI/Cu.

The isotherm constants of Equations (3) and (5) and the regression coefficient value are also summarized in Table 1.

Kinetics study

Adsorption kinetics is a useful technique to explain the type of adsorbate-adsorbent interaction and to assess the sorption mechanism. For the kinetics study, the effect of time study data was fitted into commonly used pseudo-first order and pseudo-second order rate equations. The linear form of the pseudo-first order and pseudo-second order kinetics models is respectively given in Equations (6) and (7) as under (Agarwal *et al.* 2016):

$$\ln(q_e - q_t) = \ln q_e - K_1 t \tag{6}$$

$$\frac{t}{q_t} = \frac{1}{k_2 q_{e2}} + \frac{1}{q_{e2}} t \tag{7}$$

where, q_t is the adsorption capacity at time 't' (min), q_e (mg·g^{-1}) represents adsorption capacity at equilibrium, K_1 (g·min·mg^{-1}) is the rate constant for pseudo-first order equation and K_2 (g· min·mg^{-1}) is the rate constant for the pseudo-second order equation. The plots for pseudo-first order and pseudo-second order rate equations are exhibited in the supplementary data (Figure S2(a) and S2(b)) and the values of various parameters are given in Table 2. The

Table 1 | Various parameters from Langmuir and Freundlich isotherms plot

Langmuir isotherm			Freundlich isotherm		
q_{max} (mg·g^{-1})	b (L·mg^{-1})	R^2	n	K_f (L·mg^{-1})	R^2
89.686	0.083	0.999	1.580	2.381	0.978

Table 2 | Parameters from pseudo-first order and pseudo-second order plot

Pseudo-first order			Pseudo-second order		
q_e1 (mg·g^{-1})	K_1 (g·min·mg^{-1})	R^2	q_e2 (mg·g^{-1})	K_2 (g·min·mg^{-1})	R^2
20.417	0.0780	0.938	30.48	0.434	0.999

regression coefficient (R^2) values were used to find the best fitting model. The R^2 is higher for the pseudo-second order as compared to the pseudo-first order equation. Thus, it was concluded that the sorption of Cd(II) ions STP-ZVI/Cu is well adjusted to this model, demonstrating the chemisorption mechanism (Arabkhani & Asfaram 2020).

Column test

About 2.0 gram of the adsorbent was packed in a glass tube in the form of a column. The upper and lower end of the column was protected by glass wool. 10 mL (30 mg/L, pH = 7) of Cd(II) solution was allowed to flow through the column at a flow rate 0.5 mL/min. The filtrate was collected and used for the estimation of Cd(II) having a value of 2.17 mg·L^{-1}. The removal efficiency of the adsorbent column was 92.76%. Thus, it was concluded that the adsorbent has the potential for application in water purification filters.

Regeneration of the adsorbent

Reusability is an important property of an ideal adsorbent, which reduces the overall cost of water decontamination. The current adsorbent was also regenerated and utilized. As from the pH study, the adsorbent has poor adsorption at lower pH. Therefore, the exhausted adsorbent was washed with a concentrated solution of HCl two times followed by washing with deionized water till a neutral pH. After oven drying (80 °C), the adsorption efficiency of the adsorbent was checked under optimized condition for adsorbate removal having a concentration of 30 mg·L^{-1}. The % removal was found to be 92.06% against 93.54%. The efficiency of the adsorbent has only reduced by 1.48%, ensuring the adsorbent has the capacity of reusability after elution of metal ions.

The maximum adsorption capacity of STP-ZVI/Cu is compared with some of the previously reported agricultural waste based adsorbent for Cd(II) removal from aqueous solutions as presented in Table 3. The table indicates that STP-ZVI/Cu has higher adsorption capacity for Cd(II). While, due to difference in the experimental conditions, this comparison may not be enough to decide about the superiority of the current adsorbent over the reported ones, it suggests that STP-ZVI/Cu could be an economical and potential adsorbent for Cd(II) removal from waste water. It is important to mention that non-functionalized STP was also used for the removal of Cd(II) from aqueous solutions at conditions optimized for STP-ZVI/Cu. However, the maximum adsorption capacity was 55.26 mg·g^{-1} only against 89.686 mg·g^{-1} for STP-ZVI/Cu. This result reflects the improvement in the adsorption characteristics of the functionalized spent tea over the non-functionalized spent tea.

Table 3 | Comparison of Cd(II) biosorption capacities of various adsorbents

Material	q_m (mg·g^{-1})	Reference
Salix matsudana carbon	40.98	Tang *et al.* (2017)
Raw walnut shell	7.29	Najam & Andrabi (2016)
Alkali treated walnut shell	14.29	Gondhalekar & Shukla (2015)
Banana Peels	5.91	Deshmukh *et al.* (2017)
STP	55.26	Current study
STP-ZVI/Cu	89.686	Current study

CONCLUSIONS

Zero valent Iron/Cu functionalized spent tea was prepared and characterized for the existence of various structural features necessary for metals ions uptake. The material was applied as adsorbent for the removal of Cd(II) from contaminated water. The adsorption capacity of the adsorbent was significantly influenced by parameters like pH of solution, adsorbent dosage, contact time and solution concentration. The adsorption data best fitted into the Langmuir adsorption isotherm. Similarly, the sorption process was found to occur through pseudo-second order kinetics. The material was packed into a column and successfully applied for the removal of Cd(II) from running water with removal efficiency of around 92.76%. Thus, the material has the capacity of mass scale usage for Cd(II) removal from waste water.

ACKNOWLEDGEMENTS

The authors gratefully acknowledge the research facilities provided by Centralized Resource Laboratory, University of Peshawar, Peshawar 25120, Pakistan.

CONFLICT OF INTEREST

The authors declare that there is no conflict of interest.

DATA AVAILABILITY STATEMENT

All relevant data are included in the paper or its Supplementary Information.

REFERENCES

Agarwal, S., Sadegh, H., Monajjemi, M., Hamdy, A. S., Ali, G. A. M., Memar, A. O. H., Shahryari-ghoshekandi, R., Tyagi, I. & Gupta, V. K. 2016 Efficient removal of toxic bromothymol blue and methylene blue from wastewater by polyvinyl alcohol. *Journal of Molecular Liquids* **218**, 191–197.

Ahmed, S. A., Gaber, A. A. A. & Rahim, A. M. A. 2017 Application of silica fume as a new SP-extractor for trace determination of Zn(II) and Cd(II) in pharmaceutical and environmental samples by square-wave anodic stripping vltammetry. *Applied Water Science* **7**, 677–688.

Arabkhani, P. & Asfaram, A. 2020 Development of a novel three-dimensional magnetic polymer aerogel as an efficient adsorbent for malachite green removal. *Journal of Hazardous Materials* **384**, 121394.

Bagheri, H., Afkhami, A., Saber-Tehrani, M. & Khoshsafar, H. 2012 Preparation and characterization of magnetic nanocomposite of Schiff base/silica/magnetite as a preconcentration phase for the trace determination of heavy metal ions in water, food and biological samples using atomic absorption spectrometry. *Talanta* **97**, 87–95.

Baldermann, A., Grießbacher, A. C., Baldermann, C., Purgstaller, B., Letofsky-Papst, I., Kaufhold, S. & Ietzel, M. 2018 Removal of barium, cobalt, strontium, and zinc from solution by natural and synthetic allophane adsorbents. *Geosciences* **8**, 309.

Barakat, M. A. 2011 New trends in removing heavy metals from industrial wastewater. *Arabian Journal of Chemistry* **4**, 361–377.

Deshmukh, P. D., Khadse, G. K., Shinde, V. S. & Labhasetwar, P. 2017 Cadmium removal from aqueous solutions using dried banana peels as an adsorbent: kinetics and equilibrium modelling. *Journal of Bioremediation and Biodegradation* **8**, 395.

Foo, K. Y. & Hameed, B. H. 2010 Insights into the modeling of adsorption isotherm systems. *Chemical Engineering Journal* **156**, 2–10.

Gaya, U. I., Otene, E. L. & Abdullah, A. H. 2015 Adsorption of aqueous Cd(II) and Pb(II) on activated carbon nanopores prepared by chemical activation of doum palm shell. *Springer-Plus* **4**, 458.

Gondhalekar, S. C. & Shukla, S. R. 2015 Biosorption of cadmium metal ions on raw and chemically modified walnut shells. *Environmental Progress & Sustainable Energy* **34**, 1613–1619.

Gong, T. & Tang, Y. 2020 Preparation of multifunctional nanocomposites Fe_3O_4@SiO_2-EDTA and its adsorption of heavy metal ions in water solution. *Water Science & Technology* **81**, 170–177.

Gopal, G., Sankar, H., Natarajan, C. & Mukherjee, A. 2020 Tetracycline removal using green synthesized bimetallic nZVI-Cu and bentonite supported green nZVI-Cu nanocomposite: a comparative study. *Journal of Environmental Management* **254**. https://doi.org/10.1016/j.jenvman.2019.109812.

Goyal, M., Rattan, V. K., Aggarwal, D. & Bansal, C. 2001 Removal of copper from aqueous solution by adsorption on activated carbon. *Colloids and Surfaces A Physicochemical and Engineering Aspects.* **190**, 229–238.

Gupta, V. K., Agarwal, S., Sadegh, H., Ali, G. A. M., Bharti, A. K. & Makhlouf, A. S. H. 2017 Facile route synthesis of novel graphene oxide-β-cyclodextrin nanocomposite and its application as adsorbent for removal of toxic bisphenol A from the aqueous phase. *Journal of Molecular Liquids* **237**, 466–472.

Harman, B. I. & Genisoglu, M. 2016 Synthesis and characterization of pumice-supported nZVI for removal of copper from waters. *Advances in Materials Science and Engineering*. doi:10.1155/2016/4372136.

Huang, C. C., Lo, S. L. & Lien, H. L. 2012 Zero-valent copper nanoparticles for effective dechlorination of dichloromethane using sodium borohydride as a reductant. *Chemical Engineering Journal* **203**, 95–100.

Koury, J. C., Oliveira, C. F. & Donangelo, C. M. 2007 Association between copper plasma concentration and copper-dependent metaloproteins in elite athletes. *Revista Brasileira de Medicina do Esporte* **13**, 235–238.

Lin, X. Y., Mou, R. X., Cao, Z. Y., Zhu, Z. W. & Chen, M. X. 2015 Isolation and cadmium adsorption mechanisms of cadmium-resistant bacteria strains. *Journal of Agro-Environment Science* **34**, 1700–1706.

Liu, X., Chen, Z. Q., Han, B., Su, C. L., Han, Q. & Chen, W. Z. 2018 Biosorption of copper ions from aqueous solution using rape straw powders: optimization, equilibrium and kinetic studies. *Ecotoxicology and Environmental Safety* **150**, 251–259.

Mahmoud, M. E., Amira, M. F., Abouelanwar, M. E., Seleim, S. M., Mahmoud, M. E., Amira, M. F., Abouelanwar, M. E. & Seleim, M. S. 2020 Catalytic reduction of nitrophenols by a novel assembled nanocatalyst based on zerovalent copper-nanopolyaniline-nanozirconium silicate. *Journal of Molecular Liquids* **299**, 112192.

Malook, K. & Haque, I. U. 2019 Investigation of aqueous Cr(VI) adsorption characteristics of orange peels powder. *Protection of Metals and Physical Chemistry of Surfaces* **55**, 34–40.

Mu, Y., Jia, F., Ai, Z. & Zhang, L. 2017 Iron oxide shell mediated environmental remediation properties of nano zero-valent iron. *Environmental Science: Nano* **4**, 27–45.

Najam, R. & Andrabi, S. M. A. 2016 Removal of Cu(II), Zn(II) and Cd(II) ions from aqueous solutions by adsorption on walnut

shell-Equilibrium and thermodynamic studies: treatment of effluents from electroplating industry. *Desalination and Water Treatment* **57**, 27363–27373.

Peng, S. H., Wang, R., Yang, L. Z., He, L., He, X. & Liu, X. 2018 Biosorption of copper, zinc, cadmium and chromium ions from aqueous solution by natural foxtail millet shell. *Ecotoxicology and Environmental Safety* **165**, 61–69.

Pillai, S. S., Mullassery, M. D., Fernandez, N. B., Girija, N., Geetha, P. & Koshy, M. 2013 Biosorption of Cr(VI) from aqueous solution by chemically modified potato starch: equilibrium and kinetic studies. *Ecotoxicology and Environmental Safety* **92**, 199–205.

Ponmani, S. & Udayasoorian, C. 2013 Zero valent iron (ZVI) nanocomposite for the removal of hexavalent chromium from aqueous solution. *International Journal of Engineering Science* **4**, 588–593.

Rahim, A. M. A. 2018 Apricot stone- impregnated Fe(III): an efficient, novel and eco-friendly adsorbent for removal of purpurin dye from environmental water. *Journal of Materials and Environmental Science* **9**, 444–451.

Sen, T. K., Mohammod, M., Maitra, S., Dutta, B. K., Mohammod, M., Maitra, S. & Dutta, B. K. 2010 Removal of cadmium from aqueous solution using castor seed hull: a kinetic and equilibrium study. *Clean: Soil, Air, Water* **38**, 850–858.

Sharma, S., Nagpal, K. A. & Kaur, I. 2019 Appraisal of heavy metal contents in groundwater and associated health hazards posed to human population of Ropar wetland, Punjab, India and its environs. *Chemosphere* **227**, 179–190.

Shubair, T., Eljamal, O., Khalil, A. M. E. & Tahara, A. 2018 Novel application of nanosclae zero valent iron and bimetallic nano-Fe/Cu particles for the treatment of cesium contaminated water. *Journal of Environmental Chemical Engineering* **6**, 4253–4264.

Silverstein, R. M., Webster, F. X., Kiemle, D. J. & Bryce, D. L. 2014 *Spectrometric Identification of Organic Compounds*. John Wiley & Sons, New York, NY.

Tang, C. F., Shu, Y., Zhang, R. Q., Li, X., Song, J. F., Li, B., Zhang, Y. T. & Ou, D. L. 2017 Comparison of the removal and adsorption mechanisms of cadmium and lead from aqueous solution by activated carbons prepared from *Typha angustifolia* and *Salix matsudana*. *RSC Advances* **26**, 16092–16103.

Wei, Y., Fang, Z., Zheng, L. & Tsang, E. P. 2017 Biosynthesized iron nanoparticles in aqueous extracts of *Eichhornia crassipes* and its mechanism in the hexavalent chromium removal. *Applied Surface Science* **399**, 322–329.

Wen, T., Wang, J., Li, X., Huang, S., Chen, Z., Wang, S., Hayat, T., Alsaedi, A. & Wang, X. 2017 Production of a generic magnetic Fe_3O_4 nanoparticles decorated tea waste composites for highly efficient sorption of Cu(II) and Zn(II). *Journal of Environmental Chemical Engineering* **5**, 3656–3666.

Zhang, X., Lin, S., Chen, Z., Megharaj, M. & Naidu, R. 2011 Kaolinite-supported nanoscale zero-valent iron for removal of Pb^{2+} from aqueous solution: reactivity, characterization and mechanism. *Water Research* **45**, 3481–3488.

Zuorro, A. & Lavecchia, R. 2010 Adsorption of Pb(II) on spent leaves of green and black Tea. *American Journal of Applied Sciences* **7**, 153–159.

First received 6 May 2020; accepted in revised form 21 October 2020. Available online 5 November 2020